Relaxation filtered hyperfine spectroscopy (REFINE)

Th. Maly and T.F. Prisner*

Institute of Physical and Theoretical Chemistry and Center for Biomolecular Magnetic Resonance,
Johann Wolfgang Goethe-University Frankfurt, D-60439 Frankfurt am Main, Germany

Abstract

A simple and general applicable method to separate spectrally overlapping hyperfine spectra of two paramagnetic compounds is presented. Overlapping spectral contributions from different paramagnetic species are a common situation in electron paramagnetic resonance (EPR) spectroscopy, resulting in complicate EPR spectra of metal enzymes, organic radicals or in the field of material sciences. On the other hand, the longitudinal relaxation times T_1 of these species contributing to the overall EPR signal can vary by several orders of magnitude, depending on the paramagnetic component under study. These differences can be used to selectively study individual species by using an inversion–recovery preparation sequence as a filter. Here, we demonstrate the possibility to separate hyperfine spectra of two spectrally overlapping paramagnetic species by combining an inversion–recovery based relaxation filter together with ESEEM or ENDOR hyperfine spectroscopy (REFINE). The feasibility of the presented method is demonstrated on model compounds and the necessary requirements are discussed.
© 2004 Elsevier Inc. All rights reserved.

1. Introduction

A common problem in electron paramagnetic resonance (EPR) spectroscopy is the low spectral resolution, since anisotropic interactions, especially at low temperatures, often result in broad spectra. Moreover, the presence of more than one paramagnetic species contributing to the signal, which is a typical problem in EPR spectra of biological systems or in the field of material science, often result in complex overlapping spectra. Several different techniques are available to overcome this problem. For example, differences in g values [1,2] or in the electronic spin quantum number S and m_s [3] can be used to separate diverse species.

Another possibility is the separation based on the differences in relaxation processes. For example, the observed spin–lattice relaxation times T_1 of different paramagnetic species (e.g., organic radicals, transition metal ions, and iron–sulphur clusters) can vary by several orders of magnitude [4]. In cw-EPR this offers the possibility to distinguish between each contribution by measuring the temperature and the saturation behaviour of the EPR signal.

In fact, the difference in relaxation properties can be more easily studied and exploited in time-domain techniques because the contribution of longitudinal and transversal relaxation can be separated. The stimulated echo as well as the two-pulse Hahn echo sequence provides a filter to disentangle overlapping EPR spectra by their respective longitudinal (T_1) or transversal (T_2) relaxation times. Paramagnetic species with a short T_2 relaxation time can therefore be suppressed by choosing a long pulse separation time τ in the two-pulse Hahn echo or stimulated echo experiment. If one component has a short relaxation time T_1 it is also possible to suppress it, by using a long pulse-separation time between the the second and the third pulse in the stimulated echo sequence. To suppress the long living

* Corresponding author. Fax: +49-69-798-29404.
E-mail address: prisner@chemie.uni-frankfurt.de (T.F. Prisner).
URL: www.prisner.de. ">

component it is possible to choose a shot repetition time which is shorter than the respective relaxation time T_1. These different methods have been applied to some irradiated polymers [5], as well as to biological systems [6]. However, in terms of filter design all these methods act only as a high- or low-pass filter.

To selectively suppress a single component the inversion–recovery sequence can be used since this method provides a band-pass filter. This idea adapts a technique which has been known in NMR for a long time, where the transversal as well as the longitudinal relaxation is exploited to suppress the contribution of water in 1D [7,8] and 2D [9] NMR experiments. The application of this technique to field-swept EPR and 1D-ESEEM spectroscopy was first demonstrated in 1992 [10].

Recently, we showed the application of such an inversion–recovery filter in EPR spectroscopy, to separate the field-swept and hyperfine EPR spectra of two iron–sulphur clusters of the mitochondrial respiratory protein-complex NADH:ubiquinone oxidoreductase (complex I) [11]. In this article, we want to demonstrate the generality of REFINE to separate hyperfine spectra of two overlapping species. The efficiency of the filter is experimentally demonstrated for the commonly used hyperfine spectroscopy methods electron echo envelope modulation (ESEEM) [12], hyperfine sublevel correlation (HYSCORE) [13], and electron nuclear double resonance (ENDOR) [14] and analysed numerically on the basis of simple exponential recovery functions.

2. Experimental

2.1. Sample preparation

The two well-characterised systems α,γ-bisphenylene-β-phenylallyl-benzolate (BDPA) in polystyrene (BDPA(PS)) [15] and copper-doped *l*-histidine [16,17] were used as model systems because of their overlapping EPR, but easily distinguishable hyperfine spectra to demonstrate the power of the presented method. BDPA(PS) was prepared by first solving BDPA in a solution of polystyrene in toluene. The solution was then evaporated (30 °C) and finally dried in high vacuum (10^{-5} mbar) to ensure that all solvent molecules have been removed. The final concentration for BDPA(PS) was about 5×10^{-6} mol/kg. Copper-doped *l*-histidine was prepared by adding 0.5 mol% copper(II)chloride (Fluka) to a deuterated or protonated aqueous solution of 98% pure *l*-histidine hydrochloride monohydrate (Fluka), respectively. Polycrystalline material was obtained from this solution by slow evaporation of the water over a period of a few days. The remaining material was crushed and referred to as CuHis(H) for crystals grown from the protonated solution or CuHis(D) for crystals grown from the deuterated solution.

For the mixed sample 50 mg of the respective CuHis sample was mixed together with 5 mg BDPA(PS) to achieve appropriate signal intensities.

2.2. Instrumentation

The experiments were performed on a Bruker E-580 X-band spectrometer using the Bruker dielectric cavity MD5-W1 EPR for pulsed EPR experiments and MD5EN-W1 for ENDOR experiments. The system was equipped with an Oxford helium flow cryostat (CF935) for low temperature measurements and an E-560D pulsed ENDOR accessory. Microwave pulses were amplified using a 1 kW pulsed travelling wave tube (TWT) amplifier (Applied Systems Engineering, Model 117X). Radiofrequency pulses for the ENDOR experiments were amplified by a 300 W solid state amplifier (Eni, A-300).

For ESEEM and HYSCORE experiments the lengths of the $\frac{\pi}{2}$-pulses were set to 20 ns, while a 40 ns pulse with the same amplitude was used for the π inversion pulse in HYSCORE experiments. For the REFINE preparation sequence, a 12 ns pulse was used as the π inversion pulse with an amplitude set to an optimum inversion. Unwanted contributions of echos are removed by an appropriate phase cycling sequence [18]. A set of 400 data points equally spaced by a time incrementation of 16 ns was recorded in the evolution time domain for both ESEEM and HYSCORE. For Davies-ENDOR a 200 ns π mw pulse for selective inversion of an electron spin transition was used followed by a 8 μs RF pulse. The final electron spin polarisation was monitored by the spin-echo intensity generated in a subsequent two-pulse detection sequence. A 5 μs delay was included between the RF pulse and the two-pulse detection sequence to avoid interference from RF ringdown during the two-pulse sequence.

2.3. Data processing

For background correction of the REFINE time traces (ESEEM and HYSCORE) a low-pass filtered time trace was calculated (5th order Butterworth, $\nu_{cutoff} = 0.3$ MHz) and subtracted from the experimental time trace to remove the echo decay function. Before Fourier transformation a Hanning window function was applied and the time trace was zero-filled to a total number of 512 data points. All post processing was done in Matlab. Graphical representations were made with Origin. Magnitude Fourier spectra are shown in all cases.

3. Results

The REFINE band-pass filter consists of a π inversion pulse and a filter time T_F as shown in Fig. 1. After
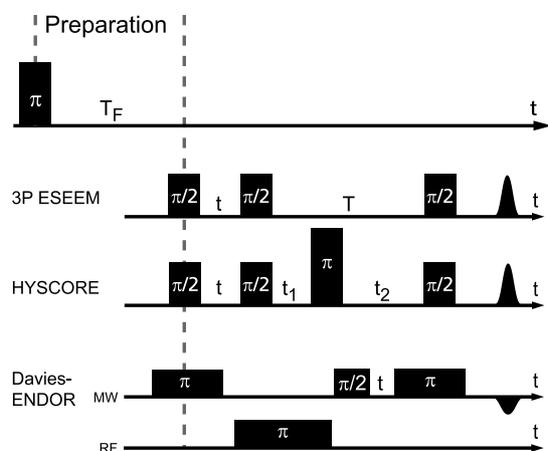
Fig. 1. Pulse sequences used in this work. The commonly used hyperfine spectroscopy methods three-pulse ESEEM, four-pulse HYSCORE, and Davies-ENDOR were combined together with an inversion–recovery preparation.

inversion of the magnetisation, every individual paramagnetic species, having a different value of T_1, will traverse its own zero-crossing point of the M_Z magnetisation, resulting in a specific filter time T_F. By choosing the two different filter times (T_F^{slow}, T_F^{fast}) and application of the respective hyperfine detection sequence at exactly these times, it is possible to separate the contributions of each individual component with respect to the complete spectrum. In this work, we chose three sequences commonly used in EPR hyperfine spectroscopy: three-pulse ESEEM, four-pulse HYSCORE, and Davies-ENDOR (Fig. 1).

Fig. 2A shows an [1]H-Davies-ENDOR spectrum of the CuHis(H)–BDPA(PS) mixture without any filter sequences applied. The spectrum is recorded at a field value corresponding to the maximum intensity of the BDPA signal ($g = 2$). Around the proton Zeeman frequency ($\nu_L(^1H) \approx 15$ MHz) the ENDOR spectrum is a rather complex superposition of proton hyperfine couplings of BDPA as well as proton and a large nitrogen hyperfine couplings of the CuHis(H) complex. To separate the hyperfine couplings belonging to the CuHis(H) complex from those arising from the BDPA(PS) the Davies-ENDOR sequence is combined with the inversion–recovery preparation as shown in Fig. 1. Two different filter times are used to disentangle the two overlapping spectra. With a filter time of $T_F = 160\,\mu s$ (10 K) an ENDOR spectrum can be recorded showing two hyperfine tensors, which can be assigned to the well known BDPA complex [15]. The assignment is done by comparing the REFINE spectrum with an ENDOR spectrum of the pure compound. Choosing a filter time of $T_F = 10$ ms these two broad features are gone and a complicate pattern of different [1]H- and ^{14}N-couplings remains. This obtained REFINE spectrum is almost identical to an ENDOR spectrum of the pure CuHis(H)
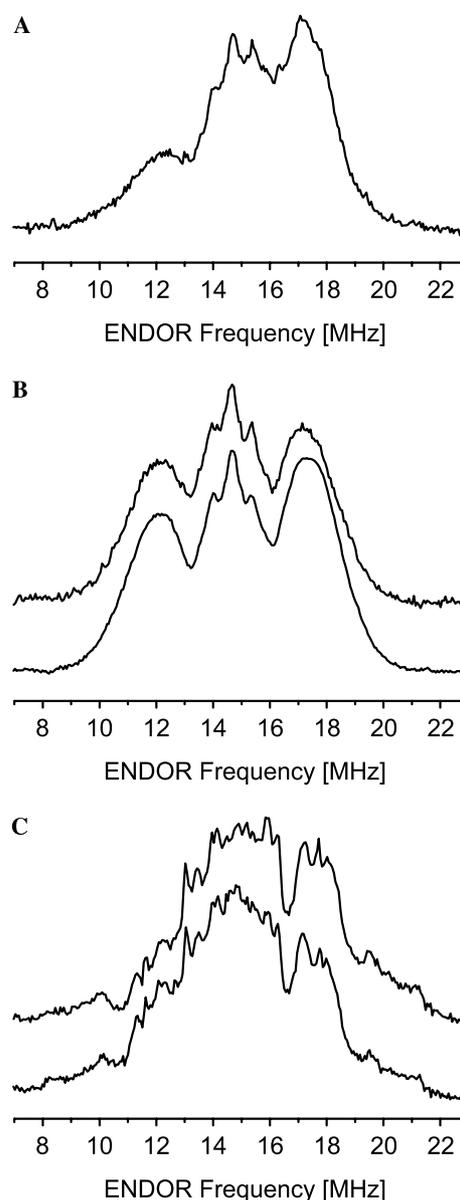

Fig. 2. Davies-ENDOR and REFINE–ENDOR applied to the CuHis(H)–BDPA(PS) mixture. To gain signal-to-noise, the experiments were performed at 10 K. The lower traces in B and C correspond to the ENDOR spectrum of the pure components. (A) Davies-ENDOR spectrum of the mixture. (B) REFINE–ENDOR with a filter time $T_F = 160\,\mu s$. (C) REFINE–ENDOR with a filter time $T_F = 10$ ms. All spectra are taken at a field value corresponding to $g = 2$. To avoid polarisation artifacts, a shot repetition time of 600 ms is used for all experiments. Ten scans are taken with a single shot per scan.

complex recorded at the same spectral position and at the same temperature. Only small variations in the amplitude can be detected but all small hyperfine couplings are still completely resolved.

For the 1D- and 2D-ESEEM experiments the CuHis system was crystallised from deuterated water. This procedure removes the water ligand and the exchangeable protons on the amine. Therefore, the ESEEM spectrum of the pure CuHis component shows almost

no modulations in the proton region (≈ 15 MHz) because remaining protons of the histidine may only have very weak intensities.

The application of REFINE–ESEEM to the model system CuHis(D)–BDPA(PS) was recently demonstrated [11]. The separation of the two major frequency contributions arising from protons of the BDPA(PS) complex (at approximately 15 MHz), and low-γ nuclei (^{2}H, ^{14}N) coordinated to the copper centre in the Cu-His(D) complex, was successfully shown. From these 1D-REFINE–ESEEM spectra the suppression efficiency was determined to be at least 85% (CuHis(D)) and 95% (BDPA(PS)).

To show that this method can also be applied to 2D-ESEEM experiments, we also recorded a REFINE–HYSCORE experiment. Fig. 3A shows the (+,+)-quadrant of the HYSCORE spectrum of the CuHis(D)–BDPA(PS) mixture. Without the filter sequence several correlations can be seen in the ^{14}N- and ^{2}H-region of the HYSCORE spectrum arising from the CuHis(D) complex as well as ^{1}H correlations for the hyperfine tensors of BDPA(PS). Using the same filter times for the REFINE–HYSCORE experiment as obtained for REFINE–ESEEM it is possible to record a HYSCORE spectrum where only the nitrogen and deuterium correlation from the CuHis(D) complex or the proton correlations of the hyperfine tensors of the BDPA(PS) are visible. The suppression of the nitrogen modulations at a filter time of $T_F^{\mathrm{CuHis(D)}} = 10$ μs is about 95% (Fig. 3B, ^{14}N). At the same filter time, as used in the 1D-ESEEM experiment to suppress the

contribution of the BDPA in the ESEEM experiment ($T_F^{\mathrm{BDPA(PS)}} = 850$ μs) almost no features are left in the corresponding HYSCORE spectrum (Fig. 3C, ^{1}H).

4. Discussion

The REFINE experiment presented, based on an inversion–recovery preparation of the spin system, is the experimental realisation of a T_1-selective band-pass filter and can be used to separate overlapping hyperfine EPR spectra from different paramagnetic species. Although the underlaying relaxation mechanisms are often complicated, resulting in non-exponential decays [4] of the inversion–recovery time traces, this does not limit the application of the presented method.

The knowledge of the respective filter times T_F^s and T_F^f is a prerequisite for the successful application of RE-FINE. The determination is straightforward in the case of isotropic T_1 relaxation, if parts of the spectra are resolved or if the relaxation behaviour can be fitted to a pure mono-exponential inversion–recovery trace as was shown previously [11]. For CuHis(D) and BDPA(PS) at a temperature of 20 K a spin–lattice relaxation time of $T_1^{\mathrm{CuHis(D)}} = 15$ μs and $T_1^{\mathrm{BDPA}} = 1.2$ ms was determined by inversion–recovery experiments (data not shown) and fitting the obtained time traces to a mono-exponential recovery function. Assuming complete inversion, this leads to filter times of $T_F^{\mathrm{CuHis(D)}} = 10.4$ μs and $T_F^{\mathrm{BDPA}} = 830$ μs. These values serve as starting points for
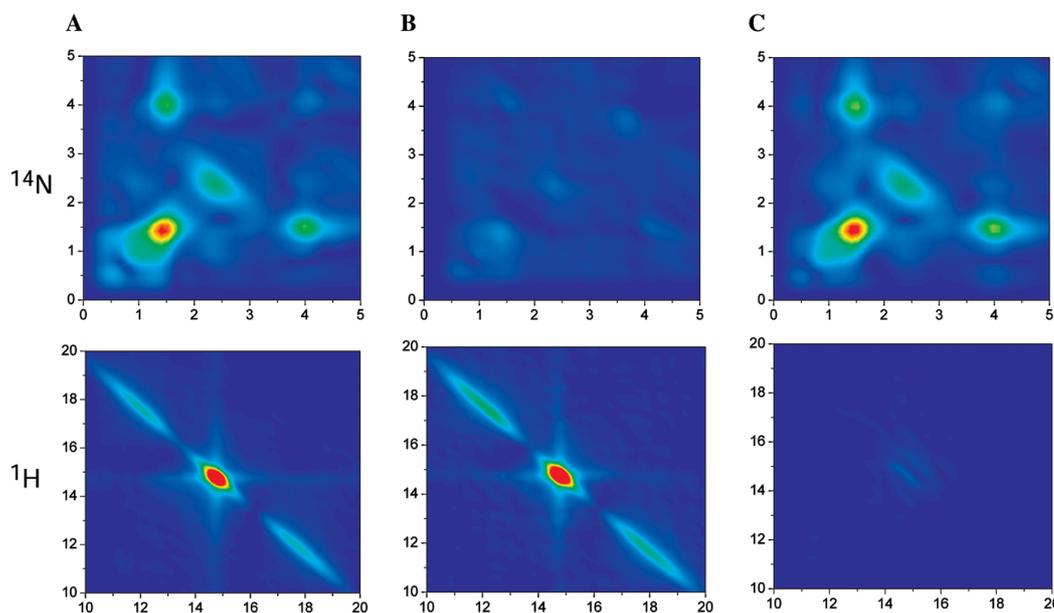

Fig. 3. REFINE–HYSCORE applied to the CuHis(D)–BDPA(PS) mixture at $T = 20K$. Only the (+,+)-quadrants are shown. Upper row, nitrogen region (0–5) MHz, lower row, and proton region (10–20) MHz. All surface plots are shown at the same contour level. (A) HYSCORE without filter sequence. (B) REFINE–HYSCORE with a filter time of $T_F = 10$ μs, (C) REFINE–HYSCORE spectrum with a filter time of $T_F = 850$ μs. All spectra are taken at a field position corresponding to $g = 2$. For all experiments, a shot repetition time of 30 ms was used and a single scans is taken with eight averages per datapoint.

a 2D search of the optimized filter times by recording field-swept spectra with different filter times T_F. Two filter times were obtained from the inversion–recovery detected field-swept spectra; $T_F = 10\,\mu s$ for suppression of the CuHis(D) signal (Fig. 4C) and $T_F = 850\,\mu s$ for suppression of the BDPA(PS) signal (Fig. 4B), which are in excellent agreement with the calculated filter times. For systems having a more complicated relaxation behaviour a complete 2D experiment (Fig. 5) has to be performed to find the optimum filter times.

As it can be seen in Fig. 4C the CuHis(D) model complex shows a slight anisotropy in T_1 across the EPR spectrum. This can be a problem when recording field-swept spectra with a fixed value of T_F. Since hyperfine spectra are recorded at a fixed field position, such field dependent anisotropy in T_1 causes no problems for the application of the presented filter sequence. From the field-swept spectra the suppression efficiency was obtained to be 98% for the CuHis(D) and 91% for the BDPA(PS) system at the respective filter times. The signal amplitudes were 91% for the CuHis(D) system and 77% for BDPA(PS) system as compared to the initial signal amplitude without inversion.

However, in most cases the hyperfine spectrum of the individual species is unknown and if the method of finding the respective filter times failed, a 2D experiment has to be performed. On the basis of the REFINE–
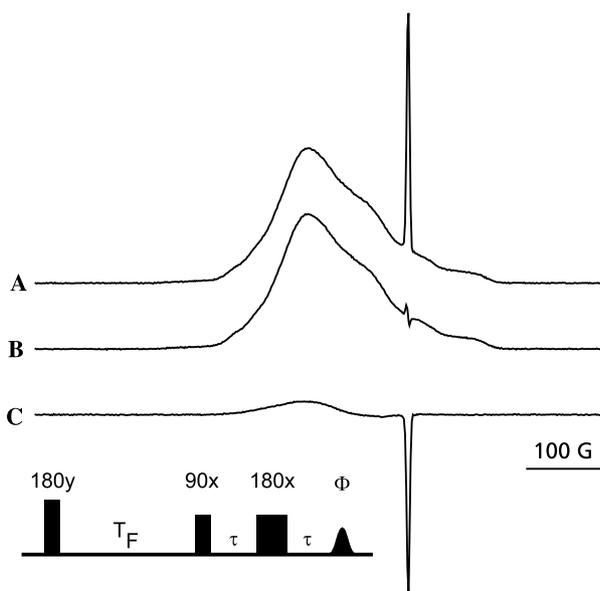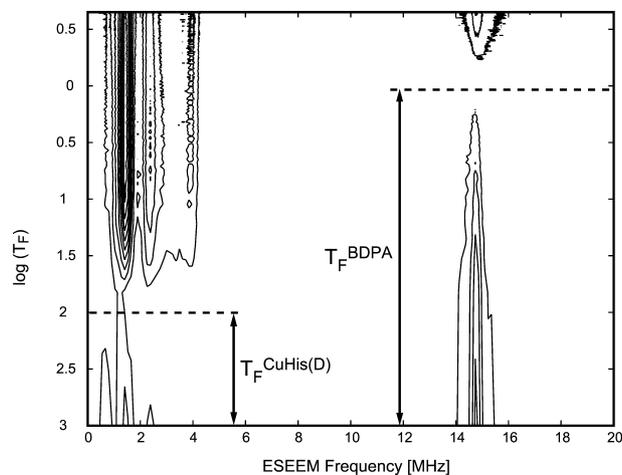

Fig. 5. Semilog contour plots of a 2D-REFINE–ESEEM experiment. The respective filter times T_F of each individual component are represented by the dashed lines. Spectra are taken at $T = 20\,K$ at a field position corresponding to $g = 2$. Experimental data are the same as for the 1D REFINE–ESEEM experiment. A total number of 300 traces are taken in the filter domain.

ESEEM sequence the strategy to determine the filter time in a 2D experiment can be demonstrated. 1D corresponds to the usually free evolution time T, under which the system is allowed to evolve under the hyperfine coupling. Fourier transformation with respect to this time increment gives the hyperfine spectra. The second dimension corresponds to the variable filter time (T_F). The obtained hyperfine spectra as a function of the filter time T_F are shown as a contour plot in Fig. 5. Both contour plots show a clear minimum in signal intensities, which are exactly corresponding to the filter times used to separate the individual contributions in the REFINE–ESEEM experiment.

To estimate the necessary requirements for a successful separation of two paramagnetic species, a simple model with mono-exponential relaxation of the slow (s) and the fast (f) relaxing component can be used. The recovery of the net magnetisation of a spin ensemble after inversion can be written as

$$M^f(t) = M_0^f \left[1 - 2a e^{-t/T_1^f} \right] \tag{1}$$

$$M^s(t) = \epsilon \cdot M_0^f \left[1 - 2a e^{-t/\gamma T_1^f} \right] \tag{2}$$

with M_0^f and T_1^f the equilibrium magnetisation and the spin–lattice relaxation time of the fast relaxing component, respectively, and a is the inversion factor, which is assumed here to be equal for both species. The equilibrium magnetisation M_0^s and the relaxation time T_1^s of the slow relaxing component are given by $M_0^s = \epsilon \cdot M_0^f$ and $T_1^s = \gamma \cdot T_1^f$, where the two parameters ϵ and γ define the ratios in intensities and decay times between the two species. From Eq. (1) it can be seen that the fast relaxing component is suppressed at the filter time

Fig. 4. Field-swept spectra of the model complex CuHis(D)–BDPA. All spectra are taken at $T = 20\,K$. The inset shows the pulse sequence used for recording the inversion–recovery detected field-swept spectra. (A) Field-swept spectrum without π inversion pulse. (B) Inversion–recovery filtered field-swept spectrum with a filter time $T_F = 850\,\mu s$. Only a neglectable contribution of the BDPA signal is left. (C) Inversion–recovery filtered field-swept spectrum with a filter time $T_F = 10\,\mu s$. The contribution of the CuHis(D) complex is completely removed at $g \approx 2$.
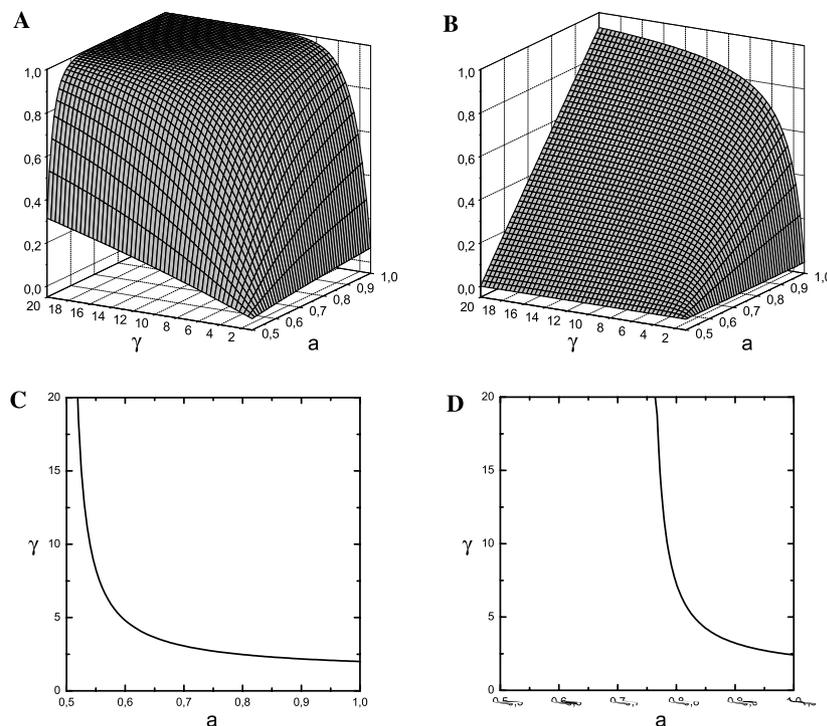
Fig. 6. Signal intensity in the REFINE experiment normalised to the equilibrium signal intensities of the species under study. Surfaces are plotted according to Eqs. (3) and (4). (A) Signal intensity of the fast relaxing component at the filter time $T_{\mathrm{F}}^{\mathrm{s}}$. (B) Signal intensity of the slow relaxing component at the filter time $T_{\mathrm{F}}^{\mathrm{f}}$. (C) Contour line at 50% signal intensity of the fast relaxing component. (D) Contour line at 50% signal intensity of the slow relaxing component.

$T_{\mathrm{F}}^{\mathrm{f}} = T_{1}^{\mathrm{f}} \cdot \ln(2a)$, while the slow component is suppressed at $T_{\mathrm{F}}^{\mathrm{s}} = \gamma \cdot T_{1}^{\mathrm{f}} \cdot \ln(2a)$. The signal intensity of the remaining species in a REFINE experiment normalised to the equilibrium signal intensity of this species is then given by:

$$M_{R}^{\mathrm{f}}(T_{\mathrm{F}}^{\mathrm{s}}) = \frac{M^{\mathrm{f}}(T_{\mathrm{F}}^{\mathrm{s}})}{M_{0}^{\mathrm{f}}} = 1 - 2a^{(1-\gamma)}, \tag{3}$$

$$M_{\mathrm{R}}^{\mathrm{s}}\left(T_{\mathrm{F}}^{\mathrm{f}}\right) = \frac{M^{\mathrm{s}}(T_{\mathrm{F}}^{\mathrm{s}})}{M_{0}^{\mathrm{s}}} = 1 - 2a^{(1-1/\gamma)}. \tag{4}$$

These two simple expressions are plotted in Figs. 6A and B. Obviously the signal intensity is larger for the fast relaxing component (Fig. 6A) compared to the slow relaxing one (Fig. 6B). On the other hand, the filter time for the suppression of the slow component ($T_{\mathrm{F}}^{\mathrm{s}}$) has not to be determined to very high accuracy. The obtained signal intensity for the slow component is more influenced by the inversion factor a and the ratio of the relaxation times (given by γ) as shown in Figs. 6C and D, where the corresponding contour line at a signal intensity of 50% compared to the pure component is plotted. From this, to achieve a signal intensity of at least 50% of the initial signal intensity of the pure component in the REFINE experiment, the inversion factor has to be $a > 0.8$ and the difference in the ratios of the relaxation times γ has to be at least 5. For systems with high signal-to-noise ratios these parameters can be smaller.

The signal intensity obtained with REFINE can be additionally compared with those obtained by other filter sequences. This was done for a stimulated echo sequence, where the fast relaxing component can be suppressed by choosing a separation time T between the second and the third pulse, which is longer than the respective relaxation time and with a fast repetition experiment, where the repetition time of the echo pulse sequence is shorter compared to the relaxation time of the slow relaxing component. By comparing the obtained signal intensities of these different experiments with those obtained by REFINE, it turned out that there is no significant loss in signal intensity by using REFINE (see Appendix A). In contrast for specific sets of parameters, the obtained signal intensity of the REFINE experiment is significantly larger.

The minimum filter time T_{F} for a very fast relaxing component is given in principle by the pulse length of the inversion pulse (16 ns in our setup), when using a phase-cycling sequence. But for such fast relaxation times no hyperfine spectra can be obtained in reality. Therefore, the minimum filter time is in the order of ≈ 200 ns.

5. Conclusions

It has been shown that REFINE spectroscopy can be used to separate the hyperfine contributions from

different paramagnetic species. This was demonstrated for the most commonly used pulsed hyperfine sequences three-pulse ESEEM, Davies-ENDOR, and four-pulse HYSCORE. As a model system, a mixture of BDPA(PS) and a CuHis complex was used. In all cases, it was possible to separate the hyperfine spectra of this two species very efficiently. The method does not require a mono-exponential longitudinal relaxation behaviour and can also be performed with field or orientation dependent relaxation times. Only a sufficient difference in the T_1 relaxation times of the two species ($\gamma > 5$) is necessary. For such systems, the method can be applied without a significant loss in sensitivity. From this, we assume that all available pulse EPR methods to study hyperfine interactions are suitable to be combined with REFINE to obtain individual hyperfine spectra in the presence of more than one paramagnetic species. Moreover, REFINE could also be capable of separating the spectral contributions of more than two species by means of an inverse Laplace transformation as it is done in diffusion ordered (DOSY) NMR spectroscopy [19]. Such experiments are currently being performed in our laboratory.

Acknowledgments

Appendix A

A filter efficiency can be defined as:

$$\mathcal{E} = \frac{\text{Rel. signal intensity of the transmitted component}}{\text{Rel. signal intensity of the rejected component}}. \quad (A.1)$$

The relative signal intensity in the REFINE experiment $M_R(T_F)$ of the transmitted signal component are shown in Fig. 6. From the experimental spectra, a very conservative relative signal intensity of the rejected component of 10% of the initial signal intensity is assumed (corresponding to 90% suppression efficiency). This leads to the following filter efficiencies for both components:

$$\mathcal{E}_R^f = 10 \cdot \frac{M_R^f(T_F^s)}{M_0^s} = 10 \cdot \epsilon^{-1}\left(1 - 2a^{(1-\gamma)}\right), \quad (A.2)$$

$$\mathcal{E}_R^s = 10 \cdot \frac{M_R^s(T_F^f)}{M_0^f} = 10 \cdot \epsilon\left(1 - 2a^{(1-1/\gamma)}\right). \quad (A.3)$$

In the following this filter efficiency will be compared to the stimulated echo sequence (for the suppression of the fast relaxing component) and to a fast repetition experiment (for the suppression of the slow relaxing component).

A.1. Suppression of the fast relaxing component

The separation time T between the second and the third pulse of the stimulated echo sequence has to be chosen larger than the respective T_1 relaxation time of the fast relaxing species. Assuming mono-exponential relaxation functions for both species the respective signal intensities are:

$$M_{SE}^f(t) = M_0^f e^{-t/T_1^f} \qquad M_{SE}^s(t) = \epsilon \cdot M_0^f e^{-t/\gamma T_1^f}. \quad (A.4)$$

To compare the filter efficiency of the three-pulse stimulated echo sequence with the REFINE experiment the signal of the slow relaxing component is calculated for a pulse separation time T, whereas the signal intensity of the fast component is reduced to 10% of its initial intensity
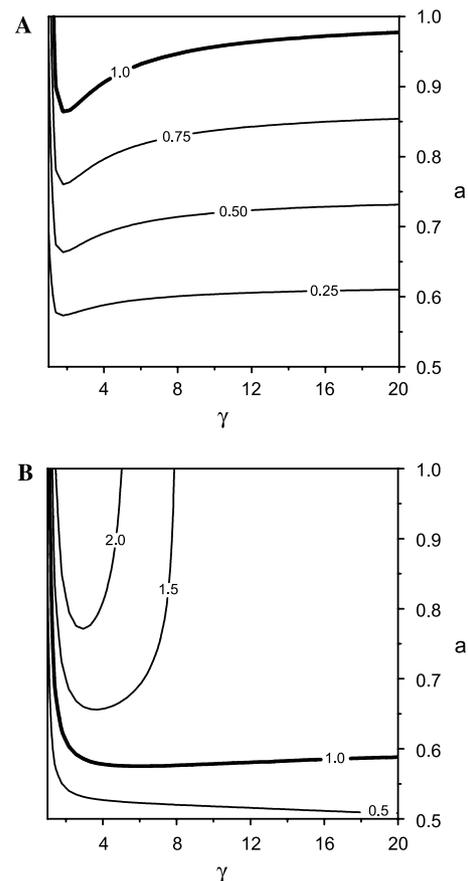

Fig. 7. Comparison of the REFINE filter efficiency with other methods. (A) Low-pass filter efficiency compared to a stimulated echo sequence; suppression of the slow relaxing component by using a long separation time T between the second and third pulse. (B) High-pass filter efficiency; suppression of the fast relaxing component under fast repetition conditions.

$$T_{SE}^f = T_1^f \cdot \ln(10) \qquad M_{SE}^s(T_{SE}^f) = \epsilon \cdot M_0^f e^{\frac{-\ln(10)}{\gamma}}. \qquad (A.5)$$

At this time T_{SE}^f the ratio of the signal intensities of the two components is given as

$$\mathcal{E}_{SE}^s = 10 \cdot \frac{M_{SE}^s(T_{SE}^f)}{M_0^f} = \epsilon \cdot 10^{(1-1/\gamma)}. \qquad (A.6)$$

The relative comparison of REFINE with the efficiency of the stimulated echo filter sequence is then given by

$$\frac{\mathcal{E}_R^s}{\mathcal{E}_{SE}^s} = \left(2a^{(1-1/\gamma)} - 1\right) \cdot 10^{(1/\gamma)} \qquad (A.7)$$

Fig. 7A shows a contour plot of (A.7). The area above the contour line at the level 1.0 indicates the region, where the efficiency obtained by REFINE compared to the stimulated echo sequence is better. What can also be seen is, that the efficiency of REFINE is mainly influenced by the inversion factor a.

A.2. Suppression of the slow relaxing component

The long living component can be suppressed alternatively by a short shot repetition time t_{SRT}, which has to be set faster than the relaxation time of the long living component. Mainly the fast relaxing component will then contribute to the obtained EPR signal. The signal intensity of the two species under fast repetition of the experiment can be expressed as [20]:

$$M_{SRT}^f(t_{SRT}) = M_0^f \cdot \frac{1 - e^{-t_{SRT}/T_1^f}}{1 + e^{-t_{SRT}/T_1^f}}, \qquad (A.8)$$

$$M_{SRT}^s(t_{SRT}) = \epsilon \cdot M_0^f \cdot \frac{1 - e^{-t_{SRT}/\gamma T_1^f}}{1 + e^{-t_{SRT}/\gamma T_1^f}}. \qquad (A.9)$$

Following the same procedure as discussed above, the time at which the signal intensity of the fast relaxing species is only 10% of the initial signal intensity is

$$T_{SRT}^s = \gamma T_1^f \cdot \ln\left(\frac{10\epsilon + 1}{10\epsilon - 1}\right), \qquad (A.10)$$

and the signal intensity of the fast relaxing component at this time is given by

$$M_{SRT}^f(T_{SRT}^s) = M_0^f \cdot \frac{1 - e^{\gamma \ln\left(\frac{10\epsilon+1}{10\epsilon-1}\right)}}{1 + e^{\gamma \ln\left(\frac{10\epsilon+1}{10\epsilon-1}\right)}}. \qquad (A.11)$$

Again, for the comparison with the REFINE experiment the ratio of the relative signal intensities of the two components at this repetition time is calculated

$$\mathcal{E}_{SRT}^f = 10 \cdot \frac{M_{SRT}^f(T_{SRT}^s)}{M_0^f} = 10 \cdot \left(\frac{1 - \left(\frac{10\epsilon-1}{10\epsilon+1}\right)^\gamma}{1 + \left(\frac{10\epsilon-1}{10\epsilon+1}\right)^\gamma}\right). \qquad (A.12)$$

The comparison of the filter efficiency of REFINE with the fast repetition experiment is then given by

$$\frac{\mathcal{E}_R^f}{\mathcal{E}_{SE}^s} = \left(1 - 2a^{1-\gamma}\right) \cdot \epsilon^{-1} \cdot \left(\frac{1 + \left(\frac{10\epsilon-1}{10\epsilon+1}\right)^\gamma}{1 - \left(\frac{10\epsilon-1}{10\epsilon+1}\right)^\gamma}\right). \qquad (A.13)$$

Fig. 7B shows a contour plot of (A.13). In comparison with the fast repetition experiment REFINE has a much better efficiency. Even for an inversion factor below 0.6, the filter efficiency is still of the same order compared to fast repetition experiment for a wide range of T_1-ratios (γ). No other experimental parameters have to be changed. From this we conclude, the signal intensities obtained with REFINE are comparable with those obtained with the stimulated echo sequence for the suppression of the fast relaxing component and are favorable compared to the fast repetition experiment in most realistic cases. Additionally, REFINE can be used in both situations and act therefore as a adjustable bandfilter, whereas the other experiments only serve for one case (low-pass or high-pass filter).

References

[1] T. Prisner, Pulsed high-frequency/high-field EPR, Adv. Magn. Opt. Res 20 (1997) 245–299.

[2] R. Eichel, A. Schweiger, Electron-Zeeman resolved paramagnetic resonance spectroscopy, J. Magn. Reson. 152 (2001) 276–287.

[3] S. Stoll, G. Jeschke, M. Willer, A. Schweiger, Nutation-frequency correlated EPR spectroscopy: the Peanut experiment, J. Magn. Reson. 130 (1998) 86–96.

[4] S. Eaton, G. Eaton, Relaxation Times of Organic Radicals and Transition Metal Ions, Ist Edition. Biological Magnetic Resonance, Kluwer Academic/Plenum Publishers, New York, 2000.

[5] H. Yoshida, T. Ichikawa, Electron spin echo studies of free radicals in irradiated polymers, Adv. Polym. Sci. 105 (1993) 3–35.

[6] C.C. Lawrence, M. Bennati, H.V. Obias, G. Bar, R.G. Griffin, J. Stubbe, High-field EPR detection of a disulfide radical anion in the reduction of cytidine 5′-diphosphate by the E441Q R1 mutant of *Escherichia coli* ribonucleotide reductase, Proc. Natl. Acad. Sci. USA 96 (1999) 8979–8984.

[7] S.L. Platt, B.D. Sykes, Water eliminated fourier transform NMR spectroscopy, J. Chem. Phys. 56 (1972) 3182–3184.

[8] J. Schulte, Sequential inversion–recovery with ride-simultaneous suppression of two solvent signals in ^{17}O M;R spectroscopy, J. Magn. Reson. 134 (1998) 168–170.

[9] A. Bax, S. Subramanian, Sensitivity-enhanced two-dimensional heteronuclear shift correlation NMR spectroscopy, J. Magn. Reson. 67 (1986) 565–569.

[10] J. Sebbach, A. Schweiger, T_1 aufgelöste EPR, oral contribution, DFG-Rundgespräch, Hirschegg, 1992.

[11] T. Maly, F. MacMillan, K. Zwicker, N. Kashani-Poor, U. Brandt, T.F. Prisner, Relaxation filtered hyperfine (REFINE) spectroscopy: a tool for studying overlapping biological EPR signals, Biochemistry 43 (2004) 3969–3978.

[12] W. Mims, Envelope modulation in spin-echo experiments, Phys. Rev. B 59 (1972) 2409–2419.

[13] P. Höfer, A. Grupp, G. Nebenführ, M. Mehring, Hyperfine sublevel correlation (HYSCPRE) spectroscopy: a 2D ESR investigation of the squaric acid radical, Chem. Phys. Lett. 132 (1986) 279–282.

[14] E.R. Davies, A new pulse ENDOR technique, Phys. Lett. A 47 (1974) 1–2.

[15] M. Bennati, C. Farrar, J. Bryant, S. Inati, V. Weis, G. Gerfen, P. Riggs-Gelasco, J. Stubbe, R. Griffin, Pulsed electron-nuclear double resonance (ENDOR) at 140 GHz, J. Magn. Reson. 138 (1999) 232–243.

[16] R. Hirasawa, H. Kon, Electron paramagnetic resonance and polarized absorption spectra of Cu(ii)-doped single crystal of *l*-histidine hydrochloride monohydrate, J. Chem. Phys. 56 (3) (1972) 4467–4474.

[17] J. Shane, P. van der Heijden, E.J. Reijerse, E. de Boer, An ESEEM investigation of single crystals and powders of copper-doped *l*-histidine hydrochloride monohydrate, Appl. Magn. Res. 6 (1994) 427–454.

[18] C. Gemperle, G. Aebli, A. Schweiger, R. Ernst, Phase cycling in pulse EPR, J. Magn. Res. 88 (1990) 241–256.

[19] C.J. Johnson Jr., Diffusion ordered nuclear magnetic resonance spectroscopy: principles and applications, Prog. NMR Spectrosc. 34 (1999) 203–256.

[20] R. Ernst, A. Wokaun, G. Bodenhausen, Principles of Nuclear Magnetic Resonance in One and Two Dimensions, International Series of Monographs on Chemistry, Oxford University Press, New York, 1989.